Volume Title
ASP Conference Series, Vol. **Volume Number**
Author
© **Copyright Year** Astronomical Society of the Pacific

arXiv:1210.0413v1 [astro-ph.HE] 1 Oct 2012

Fitting the Chandra LETG spectrum of SS Cygni in outburst with model atmosphere spectra

V.F. Suleimanov[1,2], C.W. Mauche[3], R.Ya. Zhuchkov[2], and K. Werner[1]

[1]*Institute for Astronomy and Astrophysics, Kepler Center for Astro and Particle Physics, Eberhard Karls University, Sand 1, 72076 Tübingen, Germany*

[2]*Kazan (Volga region) Federal University, Kremlevskaya str. 18, 42008 Kazan, Russia*

[3]*Lawrence Livermore National Lab., L-473, 7000 East Ave., Livermore, CA 94550, USA*

Abstract. The *Chandra* LETG spectrum of SS Cyg in outburst shows broad (≈ 5 Å) spectral features that have been interpreted as a large number of absorption lines on a blackbody continuum with a temperature of 250 kK (Mauche 2004). It is most probable that this is the spectrum of the fast-rotating optically thick boundary layer on the white dwarf surface. Here we present the results of fitting this spectrum with high gravity hot stellar model atmospheres. An extended set of LTE model atmospheres with solar chemical composition was computed for this purpose. The best fit is obtained with the following parameters: $T_{\rm eff} = 190$ kK, $\log g = 6.2$, and $N_{\rm H} = 8{\cdot}10^{19}$ cm^{-2}. The spectrum of this model describes the observed spectrum in the 60–125 Å range reasonably well, but at shorter wavelengths the observed spectrum has much higher flux. The reasons for this are discussed. The derived low surface gravity supports the hypothesis of the fast rotating boundary layer.

1. Introduction

SS Cyg is one of the best-studied cataclysmic variable stars and is a prototype of dwarf nova stars (Warner 1995). X-ray radiation of this close binary in quiescence is hard and can be described by an optically thin hot ($kT \approx 20$ keV) plasma with an observed flux $\approx 2{\cdot}10^{-10}$ erg s^{-1} cm^{-2}. In outburst, the hard X-ray flux decreases by a factor of ten, the plasma temperature is reduced to $\sim$ 6–8 keV, and an additional soft component appears with a blackbody temperature $\approx$ 200–300 kK (Córdova et al. 1980; McGowan et al. 2004; Ishida et al. 2009).

A high-resolution spectrum of the soft component was obtained with the *Chandra* LETG and was carefully investigated by Mauche (2004). The spectrum, which looks like the photospheric spectra of super-soft X-ray sources (Rauch et al. 2010; van Rossum 2012), is naturally associated with the radiation of the boundary layer (BL) between the accretion disk and white dwarf (WD) (Pringle & Savonije 1979; Kley 1991), and can be phenomenologically described by a blackbody spectrum with $T \approx 250$ kK and numerous broad absorption features of ions of O, Ne, Mg, Si, S, and Fe; the BL luminosity and WD spin were also evaluated by Mauche (2004). Here we present our attempt to fit the *Chandra* LETG spectrum of SS Cyg using the spectra of

hot stellar model atmospheres that are close to the Eddington limit, and to make more accurate estimates of the BL parameters on this basis.

2. Model atmospheres

To model high temperature atmospheres that are close to the Eddington limit, we used our version of the computer code ATLAS (Kurucz 1970), modified to deal with high temperatures (Ibragimov et al. 2003; Suleimanov & Werner 2007). We assumed local thermodynamic equilibrium (LTE) and accounted for the pressure ionization effects using the occupation probability formalism (Hummer & Mihalas 1988) as described by Hubeny et al. (1994). We took into account coherent electron scattering together with the free-free and bound-free opacity of all ions of the 15 most abundant elements using opacities from Verner & Yakovlev (1995). Line blanketing is taken into account using $\sim$ 25000 spectral lines from the CHIANTI, Version 3.0, atomic database (Dere et al. 1997).

Using our code, we calculated 22 model atmospheres with solar chemical composition. The effective temperatures of the models range between 150 kK and 250 kK with a step of 10 kK. We used two values of the surface gravity for each effective temperature: $\log g = \log g_{\rm Edd} + 0.2$ and $\log g = \log g_{\rm Edd} + 0.4$, where $\log g_{\rm Edd} = \log(\sigma_{\rm e}\,\sigma_{\rm SB} T_{\rm eff}^4/c) = 4.88 + 4\log(T_{\rm eff}/10^5\,K)$ is the surface gravity that has an equal radiation pressure force for a given $T_{\rm eff}$, and $\sigma_{\rm e} \approx 0.34$ g cm^{-2} is the electron scattering opacity for the assumed solar chemical composition. The positions of the computed models on the $T_{\rm eff}$–$\log g$ plane are shown in Fig. 1 (left panel). The considered model atmospheres are very close to the Eddington limit and a radiation pressure force $g_{\rm rad}$ due to spectral lines becomes larger than the surface gravity at the upper atmospheric layers (see Fig. 1, right panel). We did not consider moving atmospheres and we took a gas pressure equal to 10% of the total pressure ($P_{\rm gas} = 0.1 P_{\rm tot}$) if $g_{\rm rad} > g$ to enforce hydrostatic equilibrium.

Examples of the computed emergent spectra together with the temperature structures are shown in Fig. 2. The emergent spectra are dominated by absorption line forests and they become similar to the observed spectrum of SS Cyg only after accounting for the LETG spectral resolution (see Fig. 3). The differences between the spectra of models with different surface gravities is obvious (see Fig. 2, right panel) and can be found from a comparison with the observed spectrum.

3. Results

We fit the observed soft X-ray spectrum of SS Cyg using the set of model atmosphere spectra described above, convolved with the *Chandra* LETG spectral resolution $\Delta\lambda$ = 0.05 Å. The comparison of the best-fit spectrum with the observed spectrum is shown in Fig. 3, and the contours of χ^2 on the $T_{\rm eff}$–$\log N_{\rm H}$ parameter plane are shown in Fig. 4. The fitting procedure was performed in the 60–125 Å wavelength range only, because at the shorter wavelengths our model spectra cannot describe the observed spectrum. The possible reasons for this are discussed in the next section. We found that the best-fit model parameters correspond to the models with the lower surface gravity $\log g = \log g_{\rm Edd} + 0.2$ with $T_{\rm eff}$ = 190 kK, $N_{\rm H} = 8 \cdot 10^{19}$ cm^{-2}, and the normalization $K = f R_{\rm WD}^2/d^2 = 7.82 \cdot 10^{-26}$, where d is the distance to SS Cyg and f is the WD fractional

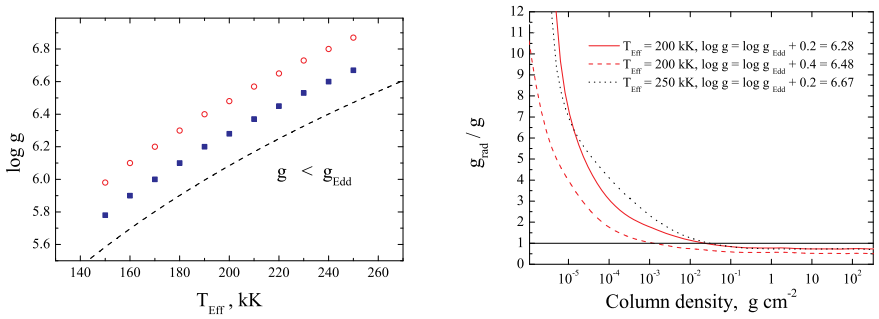


Figure 1. *Left:* Computed model atmospheres on the $T_{\rm eff}$–$\log g$ plane. The locus of points for which $\log g = \log g_{\rm Edd}$ is shown by the dashed curve. *Right:* Ratio of the radiation force to the surface gravity vs. depth for various model atmospheres.

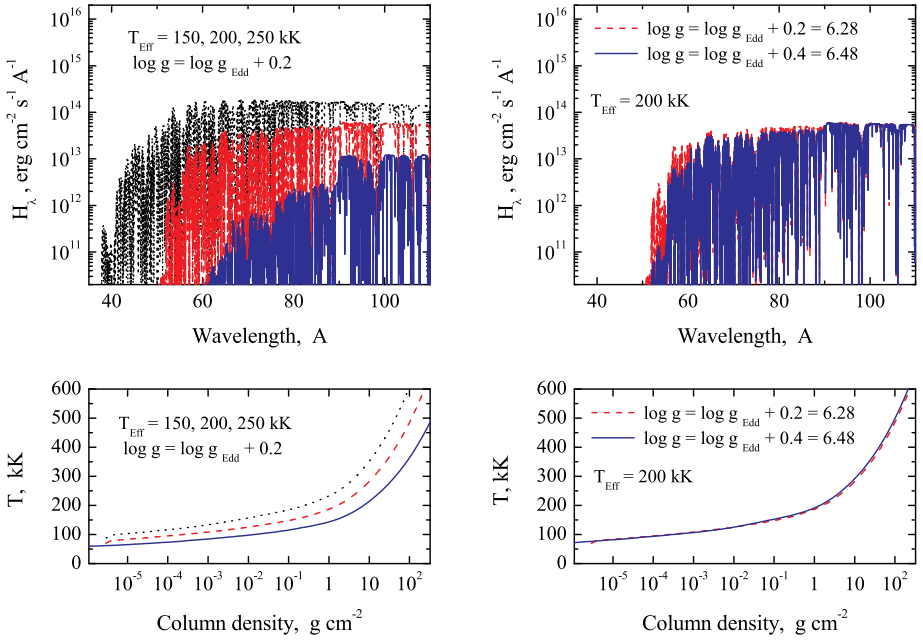


Figure 2. *Left:* Emergent spectra and temperature structures of three model atmospheres with the same differences between $\log g$ and the Eddington limit: $\log g = \log g_{\rm Edd} + 0.2$, and various effective temperatures: 150 kK (solid curves), 200 kK (dashed curves), and 250 kK (dotted curves). *Right:* Emergent spectra and temperature structures of two model atmospheres with the same effective temperature (200 kK) and different $\log g$: $\log g = \log g_{\rm Edd} + 0.2$ (dashed curves) and $\log g = \log g_{\rm Edd} + 0.4$ (solid curves).

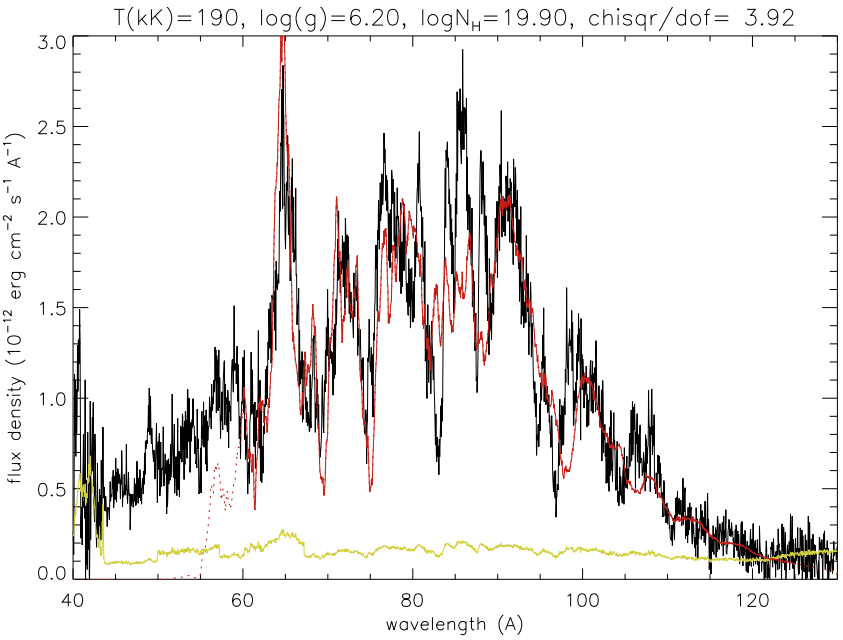


Figure 3. The *Chandra* LETG spectrum of SS Cyg in outburst (thick black curve) and the best-fit model atmosphere spectrum with $T_{\rm eff}$ = 190 kK, $\log g$ = 6.2, and $\log N_{\rm H}$ = 19.9 (thin red curve). The fitting was performed in the 60–125 Å wavelength range. The model spectrum at the shorter wavelengths is shown by the dashed curve.

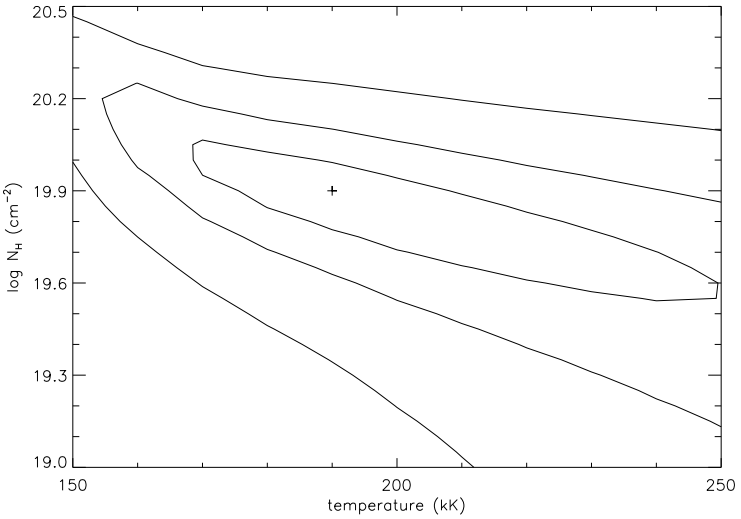


Figure 4. Position of the best-fit model on the $T_{\rm eff}$–$\log N_{\rm H}$ parameter plane and contours of $\chi^2 = [1.5, 3, 6]\chi^2_{\rm min}$.

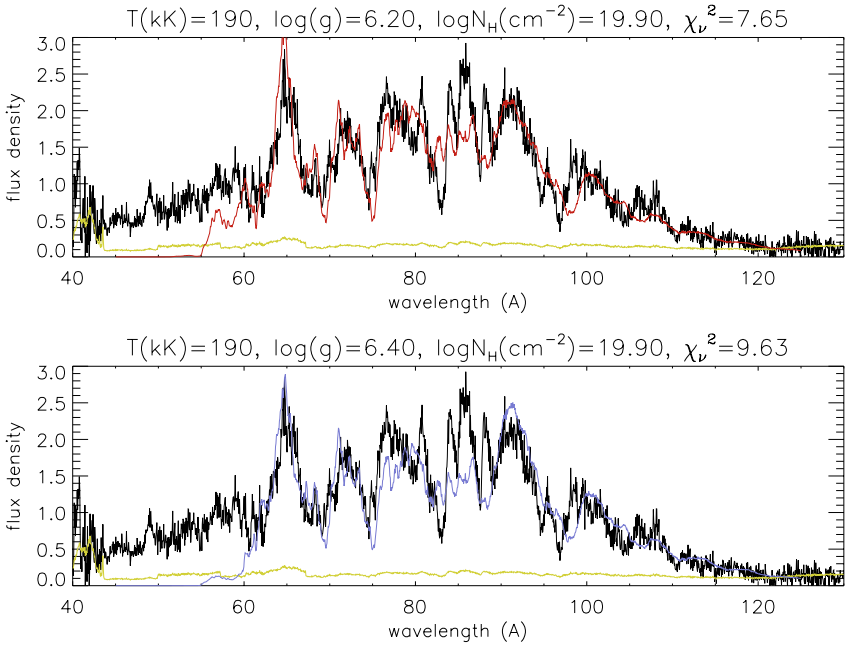


Figure 5. The *Chandra* LETG spectrum of SS Cyg in outburst (thick black curve) and best-fit model atmosphere spectra with $T_{\rm eff}$ = 190 kK, $\log N_{\rm H}$ = 19.9, and two surface gravities: $\log g$ = 6.2 (thin red curve, top panel) and $\log g$ = 6.4 (thin blue curve, bottom panel). The fitting was performed in the 45–125 Å wavelength range.

area occupied by the BL, which can be expressed as the relative BL extension along the WD surface $f \approx (2\pi R_{\rm WD}\, 2H_{\rm BL})/(4\pi R_{\rm WD}^2) = H_{\rm BL}/R_{\rm WD}$.

The obtained fit is not completely satisfactory (reduced χ^2 = 3.9), hence the formal errors are large and we have not attempted to determine them. However, the choice of the lower surface gravity is statistically justified because the reduced χ^2 is significantly larger for fits obtained using the higher gravity models ($\chi^2_{\rm d.o.f.}$ = 7.65 vs. $\chi^2_{\rm d.o.f.}$ = 9.63 for fits performed in the 45–125 Å wavelength range). This is also clear from Fig. 5, which shows that the high gravity spectrum cannot describe the local flux maxima at 78 and 92 Å.

Using the obtained fit parameters, we evaluated some basic properties of the BL. For ease of comparison, we adopted the same system and WD parameters used by Mauche (2004): $M_{\rm WD} = 1\, M_\odot$, $R_{\rm WD} = 5.5 \cdot 10^8$ cm, d = 160 pc, and an accretion disk bolometric luminosity in outburst $L_{\rm Disk} = 10^{35}$ erg s^{-1}. In this case, we can evaluate the fractional area of the BL $f = 6.3 \cdot 10^{-2}$ ($5 \cdot 10^{-3}$), the bolometric BL luminosity $L_{\rm BL} = 1.8 \cdot 10^{34}$ ($5 \cdot 10^{33}$) erg s^{-1}, and the relative BL luminosity $L_{\rm BL}/L_{\rm Disk} = 0.18\,(0.05)$, where the values obtained by Mauche (2004) are shown in parentheses. Using the well-known relation between the BL and accretion disk luminosities (Kluźniak 1987; Kley 1991) $L_{\rm BL}/L_{\rm Disk} = [1 - \Omega_{\rm WD}/\Omega_{\rm K}(R_{\rm WD})]^2$, where $\Omega_{\rm K}(R_{\rm WD})$ is the Kepler angular velocity at the WD radius, we infer that the spin period of the WD in SS Cyg is 12 (9) s.

The intrinsic surface gravity of the WD in SS Cyg ($\log g_{\rm WD} = 8.46$) is more than two orders higher than the obtained BL effective surface gravity $\log g_{\rm eff} = 6.2$. The

surface gravity of the BL can be reduced by the fast rotation of the accreting matter, and we evaluated a BL angular velocity $\Omega_{\rm BL} \approx 0.98\,\Omega_{\rm K}(R_{\rm WD})$ using the simple relation $g_{\rm eff} = g_{\rm WD} - \Omega_{\rm BL}^2 R_{\rm WD} = g_{\rm WD}\,(1 - [\Omega_{\rm BL}/\Omega_{\rm K}(R_{\rm WD})]^2)$.

4. Conclusion and Discussion

On the basis of the above analysis, we conclude that the BL in SS Cyg can be considered as a hot ($\approx$ 190 kK), fast rotating [$\Omega_{\rm BL} \approx 0.98\,\Omega_{\rm K}(R_{\rm WD})$], narrow ($H_{\rm BL} \approx 0.063\,R_{\rm WD}$) belt on the WD surface.

This deduction is founded on the fit of the SS Cyg *Chandra* LETG spectrum with the model atmosphere spectra. The obtained fit is not statistically acceptable ($\chi^2_{\rm d.o.f.} = 3.9$), especially at the shorter wavelengths (< 60 Å) and in the 82–90 Å wavelength region. These deficiencies can be connected with model shortcomings: e.g., the chemical composition may differ from solar, non-LTE effects could be important (see, e.g., Rauch et al. 2010), and the atomic data are almost certainly neither complete nor entirely accurate. The most important unmodeled effect is atmosphere expansion due to a spectral line driven stellar wind, which can be significant because $g_{\rm rad} > g$ at the outer layers of our model atmospheres (see also van Rossum 2012). It is likely that the BL cannot be described by a simple one-zone model and that it has a more complicated structure, with a distribution of effective temperatures and surface gravities over its surface. All of these effects must be taken into account in further investigations.

Acknowledgments. This work is supported by the DFG SFB / Transregio 7 "Gravitational Wave Astronomy" (V.S.) and the Russian Foundation for Basic Research (grant 12-02-97006-r-povolzhe-a) (R.Zh.). C.W.M.'s contribution to this work was performed under the auspices of the U.S. Department of Energy by Lawrence Livermore National Laboratory under Contract DE-AC52-07NA27344.

References

Córdova, F. A., Chester, T. J., Tuohy, I. R., & Garmire, G. P. 1980, ApJ, 235, 163
Dere, K. P., Landi, E., Mason, H. E., Monsignori Fossi, B. C., & Young, P. R. 1997, A&AS, 125, 149
Hubeny, I., Hummer, D. G., & Lanz, T. 1994, A&A, 282, 151
Hummer, D. G., & Mihalas, D. 1988, ApJ, 331, 794
Ibragimov, A. A., Suleimanov, V. F., Vikhlinin, A., & Sakhibullin, N. A. 2003, Astronomy Reports, 47, 186
Ishida, M., Okada, S., Hayashi, T., Nakamura, R., Terada, Y., Mukai, K., & Hamaguchi, K. 2009, PASJ, 61, 77
Kley, W. 1991, A&A, 247, 95
Kluźniak, W. 1987, Ph.D. thesis, , Stanford Univ., (1987)
Kurucz, R. L. 1970, SAO Special Report, 309
Mauche, C. W. 2004, ApJ, 610, 422
McGowan, K. E., Priedhorsky, W. C., & Trudolyubov, S. P. 2004, ApJ, 601, 1100
Pringle, J. E., & Savonije, G. J. 1979, MNRAS, 187, 777
Rauch, T., Orio, M., Gonzales-Riestra, R., Nelson, T., Still, M., Werner, K., & Wilms, J. 2010, ApJ, 717, 363
Suleimanov, V., & Werner, K. 2007, A&A, 466, 661
van Rossum, D. R. 2012, ApJ, 756, 43
Verner, D. A., & Yakovlev, D. G. 1995, A&AS, 109, 125
Warner, B. 1995, Cambridge Astrophysics Series, 28